CHEMISTRY OF MATERIALS

Article

pubs.acs.org/cm

Effect of Systematically Tuning Conjugated Donor Polymer Lowest Unoccupied Molecular Orbital Levels via Cyano Substitution on Organic Photovoltaic Device Performance

Abby Casey,[†] Stoichko D. Dimitrov,[†] Pabitra Shakya-Tuladhar,[†] Zhuping Fei,[†] Malgorzata Nguyen,[†] Yang Han,[†,‡] Thomas D. Anthopoulos,[‡] James R. Durrant,[†] and Martin Heeney*[,†]

[†]Department of Chemistry and Centre for Plastic Electronics, Imperial College London, Exhibition Road, London, SW7 2AZ, U.K.

[‡]Department of Physics and Centre for Plastic Electronics, Imperial College London, Prince Consort Road, South Kensington, London SW7 2AZ, U.K.

Supporting Information

ABSTRACT: We report a systematic study into the effects of cyano substitution on the electron accepting ability of the common acceptor 4,7-bis(thiophen-2-yl)-2,1,3-benzothiadiazole (DTBT). We describe the synthesis of DTBT monomers with either 0, 1, or 2 cyano groups on the BT unit and their corresponding copolymers with the electron rich donor dithienogermole (DTG). The presence of the cyano group is found to have a strong influence on the optoelectronic properties of the resulting donor−acceptor polymers, with the optical band gap red-shifting by approximately 0.15 eV per cyano substituent. We find that the polymer electron affinity is significantly increased by ∼0.25 eV upon addition of each cyano group, while the ionization potential is less strongly affected, increasing by less than 0.1 eV per cyano substituent. In organic photovoltaic (OPV) devices power conversion efficiencies (PCE) are almost doubled from around 3.5% for the unsubstituted BT polymer to over 6.5% for the monocyano substituted BT polymer. However, the PCE drops to less than 1% for the dicyano substituted BT polymer. These differences are mainly related to differences in the photocurrent, which varies by 1 order of magnitude between the best (1CN) and worst devices (2CN). The origin of this variation in the photocurrent was investigated by studying the charge generation properties of the photoactive polymer−fullerene blends using fluorescence and transient absorption spectroscopic techniques. These measurements revealed that the improved photocurrent of 1CN in comparison to 0CN was due to improved light harvesting properties while maintaining a high exciton dissociation yield. The addition of one cyano group to the BT unit optimized the position of the polymer LUMO level closer to that of the electron acceptor $PC_{71}BM$, such that the polymer's light harvesting properties were improved without sacrificing either the exciton dissociation yield or device V_{OC}. We also identify that the drop in performance for the 2CN polymer is caused by very limited yields of electron transfer from the polymer to the fullerene, likely caused by poor orbital energy level alignment with the fullerene acceptor ($PC_{71}BM$). This work highlights the impact that small changes in chemical structure can have on the optoelectronic and device properties of semiconducting polymer. In particular this work highlights the effect of LUMO−LUMO offset on the excited state dynamics of polymer−fullerene blends.

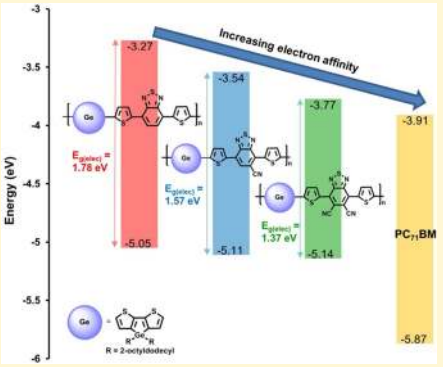

INTRODUCTION

Organic photovoltaics (OPVs) have the potential to provide low-cost energy via high throughput fabrication.[1] Large area, lightweight, and flexible devices could be produced by solution processing soluble organic semiconducting polymers using low-cost techniques such as roll-to-roll printing. The efficiency of polymer solar cells has been steadily increasing in recent years with power conversion efficiencies of single-junction cells now reaching over 10%[2−5] and tandem cells over 11%.[6,7] A particularly successful design for semiconducting donor polymers has been to incorporate both electron donating and accepting monomers into the polymer backbone.[8−10] When an electron donating monomer is copolymerized with an electron accepting monomer, the orbitals mix resulting in hybridized polymer molecular orbitals, where the polymer LUMO (lowest unoccupied molecular orbital) orbital is characteristic of the acceptor unit LUMO and the polymer HOMO (highest occupied molecular orbital) level is characteristic of the donor unit HOMO. This strategy allows for effective control of the polymer's HOMO and LUMO energy levels and therefore optical band gap. Tuning the HOMO and LUMO levels allows the short-circuit current (J_{SC}) and open-circuit voltage (V_{OC}) to be optimized for efficient OPV devices. By employing this donor/acceptor route, it has been found to be possible to

Received: May 20, 2016
Revised: July 1, 2016
Published: July 3, 2016

DOI: 10.1021/acs.chemmater.6b02030
Chem. Mater. 2016, 28, 5110−5120

reduce the LUMO level energy offset driving photoinduced charge separation to fullerene acceptor species while still maintaining reasonably efficient charge separation.[11,12] As such, donor−acceptor polymer designs often lead to increased J_{SC} through simultaneously lowering the LUMO and raising the HOMO level to reduce the polymer's band gap. However, raising the HOMO level results in a reduced V_{OC} which can impair device performance.[11,13,14] It is therefore attractive to be able to selectively stabilize the polymer LUMO level to reduce the band gap without raising the HOMO level so that an increased J_{SC} can be obtained without sacrificing V_{OC}.

Different approaches have been employed to preferentially lower polymer LUMO levels. For-instance acceptor cores such as 2,1,3-benzothiadiazole (BT)[15−17] and benzo[*d*][1,2,3]-triazole (BTz)[18] can be modified by incorporating more electronegative atoms, as in the case of thiadiazolo[3,4-*c*]pyridine (TP)[16,17,19−21] and triazolo[4,5-*c*]pyridine (TzP) (see Figure 1).[18,22,23] The free 5,6 positions of BT and BTz

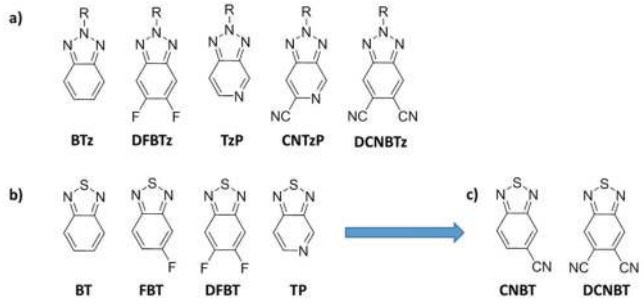

Figure 1. Chemical structures of (a) benzo[*d*][1,2,3]triazole (BTz) and derivatives and (b) 2,1,3-benzothiadiazole (BT) and derivatives with increasing electron accepting strength that have previously been used in donor−acceptor polymers for OPV applications, (c) chemical structures of monocyano and dicyano substituted BT units for use in OPV applications.

units can also be modified, for instance, with electron withdrawing fluorine substituents (see DFBTz, FBT, and DFBT in Figure 1).[24] This approach tends to lower both the HOMO and LUMO level of the polymer, leading to increased V_{OC} and therefore higher device performance.[24−26] However, the band gap of the polymer is largely unaffected as both the HOMO and LUMO are equally lowered. Despite this, many materials containing fluorinated BT still exhibit increased J_{SC}, which is usually attributed to improved charge mobility and reduced geminate recombination as opposed to increased light absorption.[26,27] The electron accepting ability of the BT core can by further increased by attaching a cyclic imide via the 5,6 positions to produce the unit 2,1,3-benzothiadiazole-5,6-dicarboxylic imide (BTI).[28] Polymers containing these units have exhibited power conversion efficiencies of over 8%.[29]

Recently the incorporation of cyano groups onto BTz[18] (see Figure 1) and thiophene[30] units in donor−acceptor polymers has been shown to stabilize LUMO levels and improve OPV performance. Cyano-substituted benzene derivatives have also been shown to have very high dipole moments.[31] The use of materials with strong dipole moments can aid charge separation in bulk heterojunction devices.[32,33] We have previously shown that including two cyano groups onto the common electron accepting monomer 4,7-di(thiophen-2-yl)-2,1,3-benzothiadiazole (DTBT) to create the monomer 4,7-di(thiophen-2-yl)-5,6-dicyano-2,1,3-benzothiadiazole (DTDCNBT) leads to a strongly stabilized LUMO level and N-type field-effect mobility when incorporated into a donor−acceptor polymer with dithienogermole (DTG) (see P(Ge-DTDCNBT) Scheme 1).[34] Continuing this theme, here we report the synthesis of the novel monocyano substituted monomer 4,7-di(thiophen-2-yl)-5-dicyano-2,1,3-benzothiadiazole (DTCNBT). We copolymerize brominated DTCNBT with DTG[35−37] to form the monocyano substituted polymer P(Ge-DTCNBT) (see Scheme 1). The optoelectronic properties and OPV device performance of P(Ge-DTCNBT) (1CN) were then compared with those of the dicyano substituted polymer P(Ge-DTDCNBT)[34] (2CN) and the polymer without cyano groups (P(Ge-DTBT) (0CN) (see Scheme 1). While we have previously reported[26] the OPV performance of P(Ge-DTBT), the OPV performance of P(Ge-DTCNBT) and P(Ge-DTDCNBT) is reported for the first time here.

Incorporating the increasingly electron withdrawing acceptor units DTBT, DTCNBT, and DTDCNBT into donor−acceptor polymers with DTG results in a series of three polymers with systematically lowered LUMO levels. We find that the polymer LUMO levels are stabilized by ∼0.25 eV upon addition of each cyano group, while the HOMO levels are weakly lowered by <0.1 eV. Power conversion efficiencies (PCE) are almost doubled from ∼3.5% to over 6.5% by adding one cyano group to the BT moiety of the polymer repeat unit but then drop to less than 1% for the polymer containing the dicyano substituted BT. The addition of one cyano group to the BT moiety optimized the position of the polymer LUMO level with respect to the LUMO level of the electron acceptor used in our study ($PC_{71}BM$), which improved the light harvesting properties of the device without sacrificing V_{OC} or photocurrent generation yields. Transient absorption spectroscopy and photoluminescence quenching studies of the P(Ge-(DTCNBT):$PC_{71}BM$ blend indicate that its exciton dissociation yields are 100% efficient regardless of the lowered LUMO level, with only a relatively small increase in geminate charge recombination compared to the higher LUMO P(Ge-DTBT) polymer, thus making this polymer the most efficient out of the series. Adding two cyano groups to the BT unit further lowers the LUMO level of the polymer, improving its device light harvesting properties but also significantly reducing J_{SC} due to inefficient exciton dissociation. We relate this to the lowering of the polymer LUMO level such that electron transfer from the polymer to the fullerene is no longer efficient. We also observe that the addition of cyano groups leads not only to polymer band gap and LUMO level reductions but also to a 120 meV reduction of their exciton binding energy, which we estimate to become as low as 0.1 eV in the dicyano substituted polymer.

Synthesis of Monomers and Polymers. The synthesis of 5-cyano-2,1,3-benzothiadiazole from 5-amino-2,1,3-benzothiadiazole via the Sandmeyer reaction has been reported previously in the literature.[38] However, to the best of our knowledge, this acceptor unit has not been incorporated into conjugated polymers. This is probably due to the harsh conditions (reflux in fuming H_2SO_4) required for the electrophilic bromination of the electron poor heterocycle which are not compatible with the nitrile group.[39] We have previously found that the fluorine substituents of 4,7-di(thiophen-2-yl)-5,6-difluoro-2,1,3-benzothiadiazole (DTDFBT) can undergo nucleophilic aromatic substitution with both thiols[40] and cyanide.[34] Encouraged by these results we investigated the substitution of the fluorine substituent in 4,7-di(thiophen-2-yl)-5-fluoro-2,1,3-benzothiadiazole

DOI: 10.1021/acs.chemmater.6b02030
Chem. Mater. 2016, 28, 5110−5120

Scheme 1. Synthetic Procedures for (a) Monomer Bis-Br(DTCNBT), (b) Monomer Bis-Br(DTDCNBT),[34] and (c) Polymers P(Ge-DTBT),[26] P(Ge-DTCNBT), and P(Ge-DTDCNBT)[34]

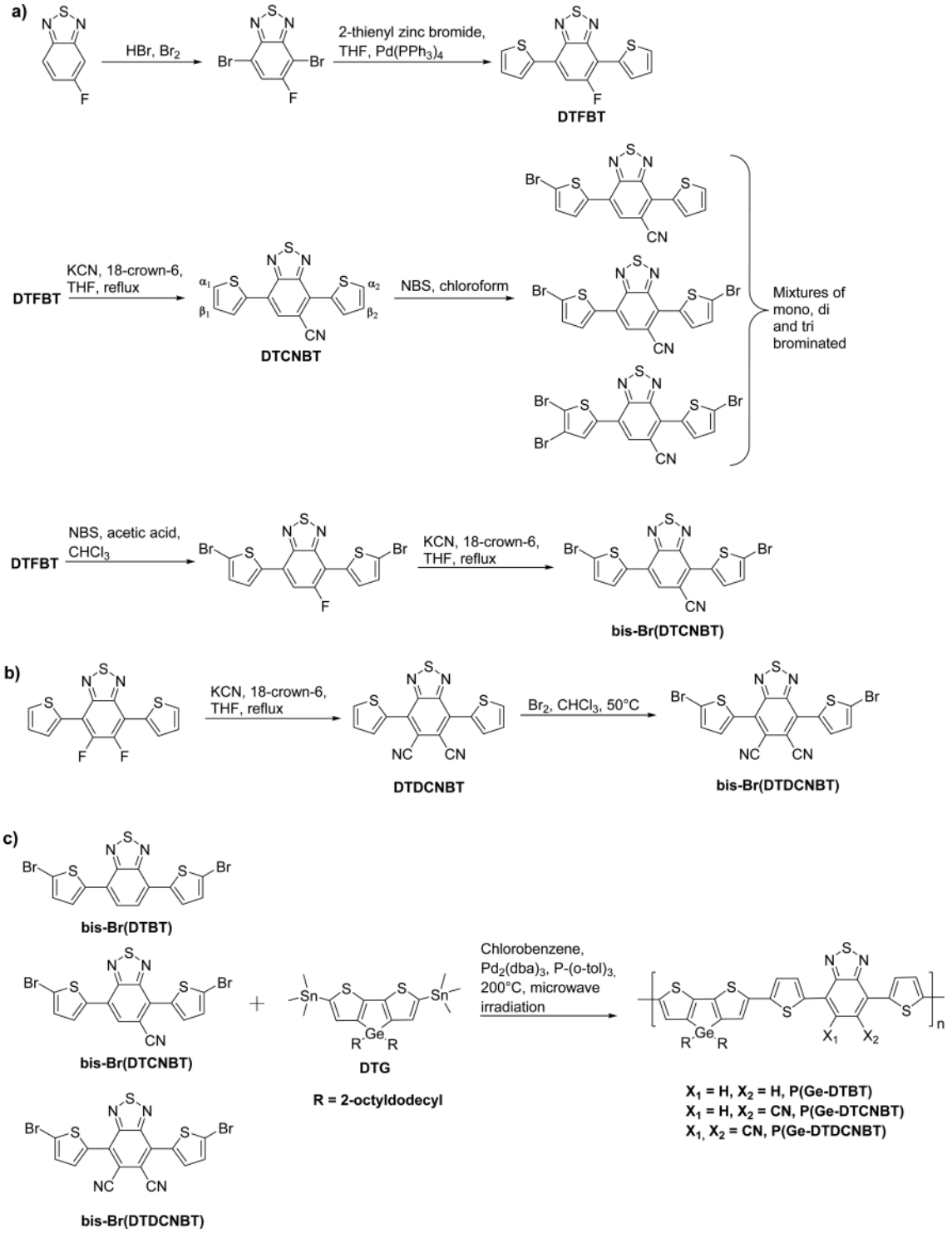

(DTFBT) using the same conditions we reported to synthesize the dicyano substituted monomer 4,7-di(thiophen-2-yl)-5,6-dicyano-2,1,3-benzothiadiazole (DTDCNBT) (Scheme 1). Under these conditions (18-crown-6, KCN, THF, reflux) the reaction proceeded much more slowly than the reaction of DTDFBT. This is likely due to the reduced electron deficiency of DTFBT over DTDFBT, reducing the rate of the initial nucleophilic attack. In contrast, the substitution of the second fluorine in DTDFBT is likely to proceed more rapidly as the first cyano group will have increased the electron deficiency of the monomer further. To increase the rate of the reaction addition of a polar aprotic cosolvent DMF was successful and the reaction was complete after 12 h. The mono cyanated product 4,7-di(thiophen-2-yl)-5-cyano-2,1,3-benzothiadiazole DTCNBT was obtained in similar yield (~70%) to that we reported for DTDCNBT (76%) (see Scheme 1). However, unlike DTDCNBT the subsequent bromination of DTCNBT proved problematic.

DOI: 10.1021/acs.chemmater.6b02030
Chem. Mater. 2016, 28, 5110−5120

Bromination of DTDCNBT required heating in excess bromine due to the reduced reactivity of the α_1 and α_2 positions (see Scheme 1b). Both of these positions are less reactive in comparison to DTDFBT due to the strongly electron withdrawing cyano groups reducing the electron density at these positions. However, the α_1 and α_2 positions of DTCNBT have differing reactivity, with the α_1 position having a higher reactivity in comparison to the α_2 position closer to the cyano group (Scheme 1a). Initially, to avoid brominating the β_1 position of DTCNBT 2 equiv of NBS in chloroform were used instead of excess molecular bromine. However, the reaction proceeded very slowly and afforded a mixture of starting material and singly brominated product, presumably brominated in the α_1 position. Gently heating the solution led to an increased quantity of the monobrominated product; however, no dibrominated product was formed. Addition of a further 2 equiv. of NBS and further heating lead to a complex mixture of mono, di, and tribrominated products. It is likely that the strongly electron withdrawing cyano group reduces the reactivity of the α_2 position, so that the α_2 and β_1 position are now a similar reactivity. We were unable to separate the mono, di, and tribrominated products by column chromatography or recrystallization.

As a solution to these difficulties, the cyanide substitution reaction was investigated on the dibrominated DTFBT. Previously we had found that some substitution of the thienyl bromide was observed when using strong nucleophiles (thiols) under S_NAr conditions.[40] However, the reaction proceeded cleanly with cyanide as the nucleophile, and dibrominated monomer bis-Br(DTCNBT) was obtained in relatively high yield (76%) after recrystallization from chloroform (see Scheme 1a). We note that Marder and co-workers[41] have recently demonstrated an alternative procedure whereupon bromoarenes such as 2-bromo-5-trimethylsilylthiophene can be coupled to the DCNBT unit via palladium-catalyzed C−H direct arylation.

We have previously reported the synthesis of the polymers P(Ge-DTDCNBT)[34] and P(Ge-DTBT)[26] along with the constituent acceptor monomers bis-Br(DTDCNBT)[34] (see Scheme 1b) and bis-Br(DTBT)[26] and donor monomer 4,4-bis(2-octyldodecyl)-5,5-bis(trimethyltin)-dithieno[3,2-b:2,3-d]-germole[26] (DTG, Scheme 1c). The long and bulky 2-octyldodecyl side chains are necessary to ensure sufficient polymer solubility. All polymers were synthesized via microwave-assisted Stille coupling.[42] The molecular weights of the polymers after Soxhlet purification were determined by gel permeation chromatography in chlorobenzene at 80 °C (see Table 1). While the molecular weight of P(Ge-DTDCNBT) is somewhat lower than both P(Ge-DTBT) and P(Ge-DTCNBT), we believe it to be sufficiently high to be in the plateau region in terms of molecular properties.

Optical Properties. The absorption spectra of P(Ge-DTBT), P(Ge-DTCNBT), and P(Ge-DTDCNBT) in both chlorobenzene solution and thin film are shown in Figure 2, and the optical properties are summarized in Table 1. P(Ge-DTBT) has an absorption maximum (λ_{max}) at 665 nm in solution and 676 nm in thin film, giving a small red shift of 11 nm as the polymer enters the solid state. The addition of one cyano group to each BT unit in P(Ge-DTCNBT) led to highly red-shifted absorptions in comparison to P(Ge-DTBT). P(Ge-DTCNBT) has a λ_{max} at 735 nm in solution and 786 nm in thin film, resulting in a significant red shift of 110 nm compared to the film of P(Ge-DTBT). The 51 nm red-shift upon film formation and the appearance of a shoulder at ∼728 nm in thin film suggest strong aggregation in the solid state.

Table 1. Molecular weights and optical properties of P(Ge-DTBT), P(Ge-DTCNBT) and P(Ge-DTDCNBT)

polymer	M_n (kDa)[a]	M_w (kDa)[a]	Đ	$\lambda_{abs,max}$ nm (sol)[b]	$\lambda_{abs,max}$ nm (film)	$E_{g(opt)}$[c] eV
P(Ge-DTBT)	39.0	97.5	2.5	665	676	1.56
P(Ge-DTCNBT)	42.0	109.2	2.6	735	786	1.40
P(Ge-DTDCNBT)	20.5	44.4	2.2	754	833	1.27

[a]Molecular weights measured using gel permeation chromatography (against polystyrene standards) in chlorobenzene at 80 °C. [b]Determined from solution UV−vis absorption spectroscopy in chlorobenzene. [c]Determined from the absorption onset of the polymers in thin film.

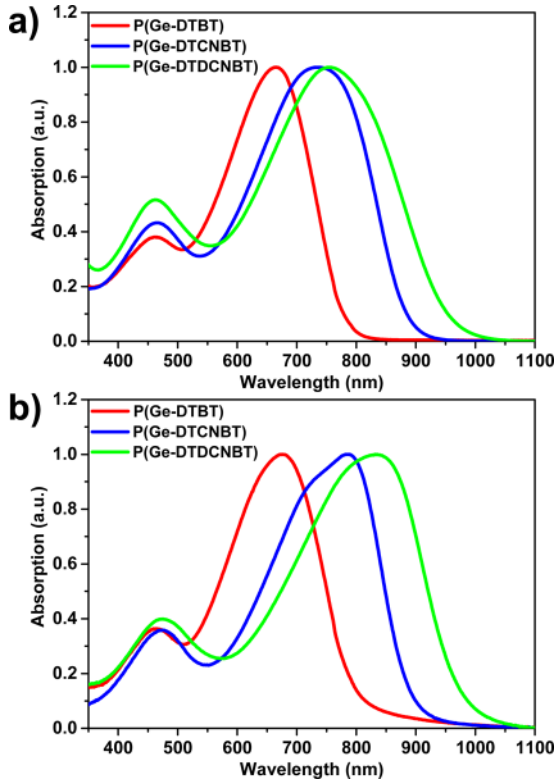

Figure 2. UV−vis spectra of P(Ge-DTBT), P(Ge-DTCNBT), and P(Ge-DTDCNBT) in (A) chlorobenzene solution and (B) thin film.

The addition of two cyano groups to each BT unit in P(Ge-DTDCNBT) leads to further red shifts in both solution and thin film in comparison to P(Ge-DTBT) and P(Ge-DTCNBT). P(Ge-DTDCNBT) has an absorption maximum at 754 nm in solution and 833 nm in thin film, giving a large red shift of 79 nm as the polymer enters the solid state. The λ_{max} of P(Ge-DTDCNBT) in thin film is red-shifted by 157 nm in comparison to the film of P(Ge-DTBT).

The solid state absorption spectra (see Figure 2), in which all the polymers are likely to be more coplanar, show a sequential red-shift in absorption maxima as the electron deficiency of the acceptor unit is increased. These red-shifts in absorption translate into reduced optical band gaps, which were measured from the absorption onset of the polymers in thin film. The optical band gaps of the polymers reduce sequentially as the electron deficiency of the acceptor unit is increased (see

DOI: 10.1021/acs.chemmater.6b02030
Chem. Mater. 2016, 28, 5110−5120

Table 1). The optical band gap is reduced by 0.16−0.17 eV upon addition of each cyano group to the repeat unit of the polymer.

Electrochemical Properties. To investigate the origin of the reduction in optical band gap observed as the strength of the electron accepting moiety in the polymer is increased, the energy levels of the polymers were investigated as thin films using cyclic voltammetry (CV) and photoelectron spectroscopy in air (PESA). The cyclic voltammograms of the three polymers are shown in Figure 3 and the electronic properties of all three

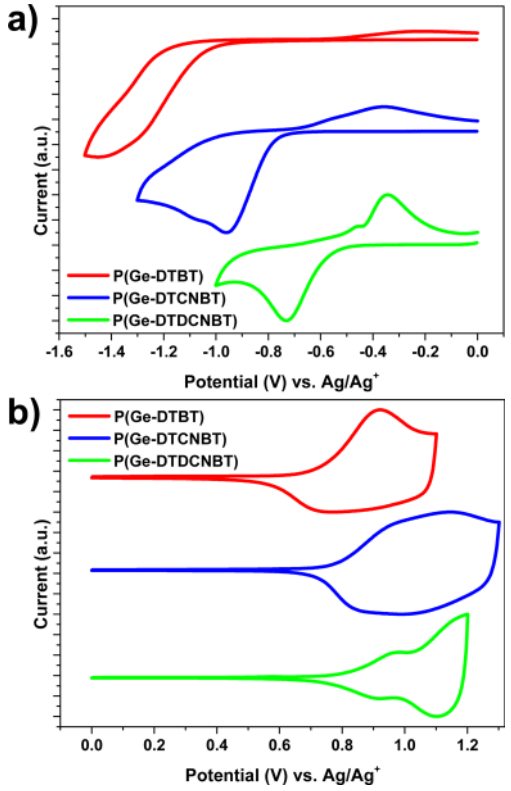

Figure 3. Cyclic voltammograms of (A) the reduction cycles and (B) the oxidation cycles of thin films of P(Ge-DTBT), P(Ge-DTCNBT), and P(Ge-DTDCNBT) in acetonitrile−[n-Bu_4N]PF_6 solutions (0.1 M) at a scan rate of 100 mV s^{-1}.

polymers are summarized in Table 2. The HOMO and LUMO levels of the polymers were estimated from the onset of first oxidation and the onset of the first reduction, respectively, assuming the ferrocene/ferrocenium reference to be 4.8 eV below the vacuum level.[43] The HOMO levels of the polymers were also estimated by measuring the ionization potential of polymer thin films using PESA. Both methods for estimating the HOMO levels of the polymers show a steady stabilization of the HOMO level with addition of cyano groups to the BT moiety of the repeat unit although the absolute levels are different. The HOMO levels of P(Ge-DTBT), P(Ge-DTCNBT), and P(Ge-DTDCNBT) were estimated to be −5.05 eV, −5.11 eV, and −5.14 eV, respectively, from CV measurements. The HOMO level was therefore reduced (i.e., moved further from the vacuum level) by approximately 0.05 eV upon addition of each cyano group to the BT moiety in each polymer repeat unit.

PESA measurements showed slightly larger shifts in the HOMO energies of approximately 0.1 eV per cyano group (see Table 2). Both CV and PESA measurements estimate similar HOMO level energies/ionization potentials for P(Ge-DTBT) and P(Ge-DTCNBT). However, for P(Ge-DTDCNBT) PESA measurements estimate the HOMO level to be deeper (−5.30 eV) than that estimated using CV measurements (−5.14 eV). It should be noted that PESA measurements have an associated error of ±0.05 eV and CV measurements can have errors of over ±0.1 eV, particularly when thin films of the materials are deposited onto the working electrode, as is the case in this work.[44] CV measurements therefore cannot accurately estimate changes in the energy levels of less than 0.1 eV. It is therefore important to combine both techniques in order to get a more accurate representation of the energy levels. Using both techniques and taking into account these errors it appears that the HOMO level is weakly stabilized by ∼0.1 eV with each additional cyano group.

In comparison, the LUMO levels estimated using the reduction potential measured by CV are more strongly stabilized upon addition of cyano groups to the BT unit than the HOMO levels. The LUMO levels of P(Ge-DTBT), P(Ge-DTCNBT), and P(Ge-DTDCNBT) were estimated to be −3.27 eV, −3.54 eV, and −3.77 eV, respectively, using CV measurements. The LUMO levels were therefore lowered by approximately 0.25 eV upon addition of each cyano group to the repeat unit of the polymer. Because of the larger effect on the LUMO level the electrochemical band gap ($E_{g(elec)}$) is sequentially lowered by around 0.2 eV per cyano substituent.

The energy levels of the polymers estimated using cyclic voltammetry are plotted in Figure 4. Often polymer LUMO levels are estimated by adding the optical band gap ($E_{g(opt)}$) to the ionization potential measured using PESA. However, the optical band gap does not take into account the exciton binding energy.[45] As can be seen in Table 2 "LUMO levels" estimated using this method are therefore approximately 0.2 eV deeper than those estimated using CV. While this method is an inaccurate way to measure the absolute value of the LUMO level, the difference between the LUMO levels of the polymers measured using this method should be accurate. This method

Table 2. Electronic Properties of P(Ge-DTBT), P(Ge-DTCNBT), and P(Ge-DTDCNBT)

material	HOMO,[a] eV	LUMO,[a] eV	$E_{g\ (elec)}$, eV[a]	$E_{BE,}$ eV[b]	I.P., eV (PESA)[c]	"LUMO"[d], eV (I.P. + $E_{g\ (opt)}$)	DFT, HOMO[e]	DFT, LUMO[f]
P(Ge-DTBT)	−5.05	−3.27	1.78	0.22	5.04	−3.47	−4.80	−3.28
P(Ge-DTCNBT)	−5.11	−3.54	1.57	0.17	5.15	−3.75	−4.99	−3.63
P(Ge-DTDCNBT)	−5.14	−3.77	1.37	0.10	5.30	−4.03	−5.20	−3.91

[a]HOMO, LUMO, and $E_{g(elec),}$ electrochemical band gap, determined by thin film cyclic voltammetry referenced to ferrocene/ferrocenium at −4.8 eV, error associated with measurement is ±0.1 eV.[44] [b]E_{BE}, the exciton binding energy, calculated from the difference of electronic and optical band gaps ($E_{g(elec)} - E_{g(opt)}$). $E_{g(opt)}$ is taken from Table 1. [c]Determined by photoelectron spectroscopy in air (PESA) on thin films, error associated with measurement ± 0.05 eV. [d]Estimated by adding $E_{g(opt)}$ to the negative of the ionization potential determined by PESA. [e]Calculated using DFT with a B3LYP functional and basis set of 6-311g(d). [f]Calculated using TD-DFT with a B3LYP functional and basis set of 6-311g(d).

DOI: 10.1021/acs.chemmater.6b02030
Chem. Mater. 2016, 28, 5110−5120

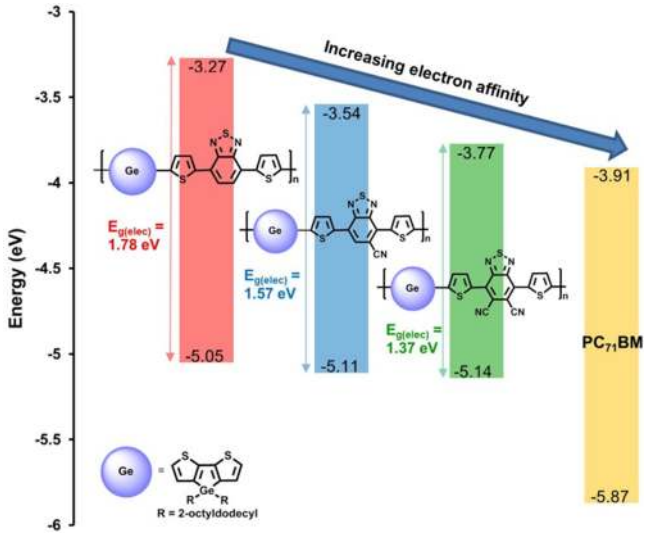

Figure 4. Thin film energy levels of P(Ge-DTBT) (red), P(Ge-DTCNBT) (blue), and P(Ge-DTDCNBT) (green) measured using cyclic voltammetry and plotted against $PC_{71}BM$ (yellow) energy levels obtained from literature cyclic voltammetry measurements.[46]

showed that each cyano group stabilized the LUMO by 0.28 eV, in good agreement with the CV measurements despite differences in the absolute energies estimated using both methods. The increases in electron affinity upon addition of each cyano group are well above the errors associated with each technique.

HOMO and LUMO energies were estimated using DFT and TD-DFT (time-dependent density functional theory), respectively, (B3LYP functional with basis set of 6-311G(d)). Calculations were formed on trimer oligomers with methyl groups instead of the full solubilizing groups in order to simplify calculations. Calculated HOMO and LUMO energies broadly agree with the trend shown by both PESA and CV measurements (see Table 2), showing a stronger stabilization of the LUMO level (~0.3 eV per cyano group) in comparison to the HOMO level (~0.2 eV per cyano group).

Comparison of the magnitudes of the electronic and optical band gaps allows us to estimate the exciton binding energy, $E_{BE} = E_{g(elec)} - E_{g(opt)}$), as listed in Table 2. It is apparent that each cyano substituent results in a significant reduction in binding energy, with an overall 120 meV reduction for P(Ge-DTDCNBT) compared to P(Ge-DTBT). This reduction in binding energy may be associated with the increased localization and spatial separation of the HOMO and LUMO orbitals with cyano substitution (see Figure 5), as discussed below. The intramolecular dipole associated with intramolecular charge transfer is also likely to increase with increasing electron accepting strength, which has been suggested to reduce exciton binding energies.[32] We also note that these estimated binding energies, while difficult to quantify in absolute terms, are relatively small, ranging from 220 to 100 meV, indicative of relatively facile charge separation from polymer excitons.

Optimized Polymer Geometries and Molecular Orbitals. The optimized geometries and molecular orbital distribution of the polymers were calculated using DFT with the B3LYP level of theory and a basis set of 6-311G(d) and are shown in Figure 5. Calculations were carried out on trimers of the repeat units with methyl groups instead of the full alkyl chains to simplify calculations. It is not surprising that modification of the BT unit with cyano groups predominantly affects the energy of the LUMO level since the wave function of the LUMO level is concentrated on the BT unit (see Figure 5). It is also clear from the molecular orbital plots that while the HOMO level remains delocalized along the polymer backbone for all three polymers, the LUMO level becomes gradually more localized onto the BT unit as cyano groups are added. The LUMO level of P(Ge-DTBT) is the most delocalized, while the LUMO level of P(Ge-DTDCNBT) is the least delocalized (see Figure 5).

In agreement with literature calculations performed on the monomer DTBT,[25] we found that in the lowest energy conformation of P(Ge-DTBT) the thiophene units are roughly planar and trans to the BT unit, i.e., thiophene sulfur atoms pointing in the opposite direction to the BT sulfur. However, in the lowest energy conformation of P(Ge-DTDCNBT) the

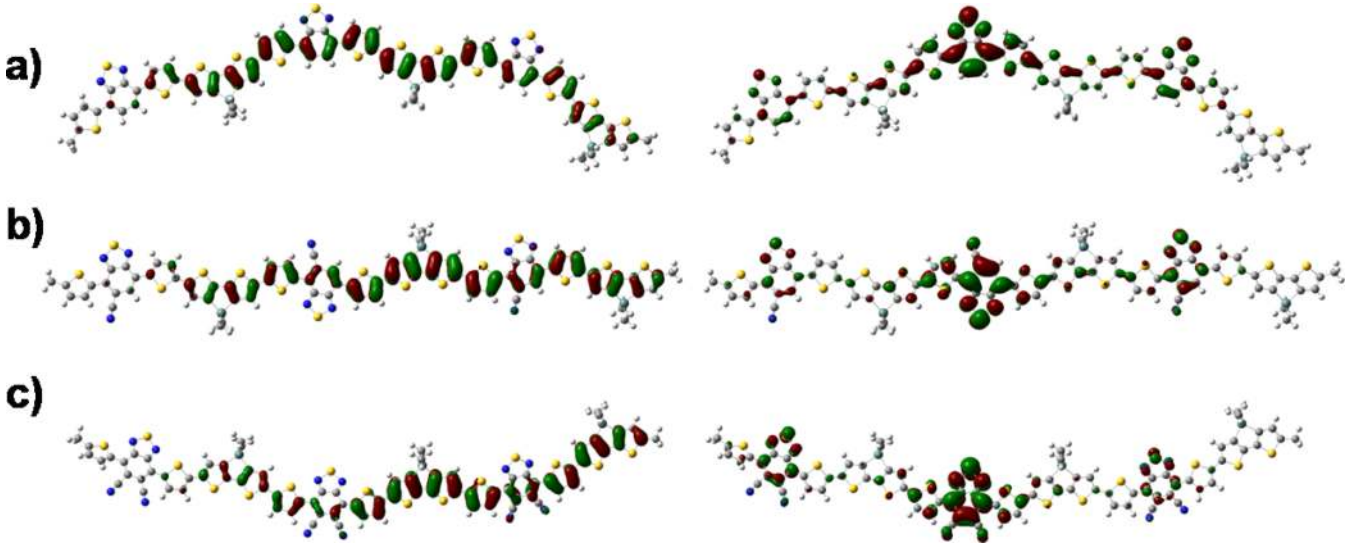

Figure 5. HOMO (left) and LUMO (right) electron density plots and optimized geometries for (A) P(Ge-DTBT), (B) P(Ge-DTCNBT), and (C) P(Ge-DTDCNBT) calculated using DFT with a B3LYP functional and basis set of 6-311G(d).

DOI: 10.1021/acs.chemmater.6b02030
Chem. Mater. 2016, 28, 5110−5120

Table 3. Summary of Photovoltaic (1:2 Ratio of Polymer:$PC_{71}BM$) and Field-Effect Transistor Device Performance

					mobility (cm^2V^{-1} s^{-1})[c]	
polymer	$J_{SC\ (max)}$ ($J_{SC\ (average)}$) (mA cm^{-2})	$V_{OC\ (max)}$ ($V_{OC\ (average)}$) (V)	FF_{max} ($FF_{average}$)	PCE_{max} % ($PCE_{average}$)	holes	electrons
P(Ge-DTBT)[a]	7.95 (7.45 ± 0.5)	0.66 (0.65 ± 0.01)	0.68 (0.66 ± 0.02)	3.51 (3.35 ± 0.20)	2.2×10^{-3}	n/a
P(Ge-DTCNBT)[a]	14.83 (13.72 ± 1.1)	0.68 (0.67 ± 0.01)	0.70 (0.65 ± 0.06)	6.55 (6.03 ± 0.65)	2.5×10^{-2}	n/a
P(Ge-DTDCNBT)[b]	2.99 (2.42 ± 0.5)	0.68 (0.49 ± 0.24)	0.36 (0.32 ± 0.05)	0.63 (0.39 ± 0.25)	n/a	2.8×10^{-3}

[a]Top gate/bottom contact OFET devices made with gold electrodes treated with PFBT. [b]Top gate/bottom contact OFET devices made with untreated gold electrodes. [c]Peak charge carrier mobilities calculated in saturation regime.

thiophene units are ~25° out of plane and cis to the BT unit, i.e., thiophene sulfur atoms pointing in the same direction as the BT sulfur. The significant dihedral angle between the thiophene and BT unit is caused by steric clash with the cyano groups. Single crystal analysis of the DTDCNBT unit, carried out previously,[34] confirmed the preferred cis structure with roughly 30° dihedral angle between the thiophene and DCNBT unit. As expected in the lowest energy conformation of P(Ge-DTCNBT), the thiophene adjacent to the cyano group on the BT unit is out plane (~20 °C) and in a cis conformation while the thiophene adjacent to the hydrogen on the BT unit is almost planar and in a trans conformation. This alternating cis, trans pattern of the thiophenes leads to a more linear polymer conformation, as can be seen from the modeled trimer in Figure 5b. Even though P(Ge-DTCNBT) is expected to be a regiorandom polymer with respect to the orientation of the cyano groups, the alternating cis, trans pattern of thiophene still leads to a more linear backbone irrespective of the relative orientation of the CNBT unit.

OPV Device Performance. We have previously investigated the OPV device performance of P(Ge-DTBT) and found that a 1:2 blend ratio of polymer:$PC_{71}BM$ in *o*-DCB (*ortho*-dichlorobenzene) gave optimal device performance.[26] A polymer:$PC_{71}BM$ blend ratio of 1:2 in *o*-DCB was therefore used to investigate the photovoltaic performance of both P(Ge-DTCNBT) and P(Ge- DTDCNBT).

The photovoltaic performance of P(Ge-DTCNBT) and P(Ge-DTDCNBT) in a device configuration of glass/ITO/PEDOT:PSS/polymer:$PC_{71}BM$/Ca/Al were measured, while the charge transport properties of all three polymers were tested in organic field-effect transistor (OFET) devices in the top gate, bottom contact device configuration. The OPV and OFET device performances of the polymers are summarized in Table 3. The transfer and output characteristics of all three polymers can be seen in Figure S3, and the UV absorption spectra of the blend films are shown in Figure S4. Figure 6 shows the *J*−*V* curves for the best devices made from 36 mg/mL solutions of polymer and $PC_{71}BM$ (1:2) with a blend ratio of 1:2 in *o*-DCB solutions. As expected from the relatively similar polymer HOMO levels, the peak open circuit voltages (V_{OC}) of the devices made from the different polymers varied little. P(Ge-DTDCNBT) and P(Ge-DTCNBT) exhibited slightly higher peak open circuit voltages than P(Ge-DTBT) (0.68 V in comparison to 0.65 V), as expected as their HOMO levels are weakly lowered by the addition of one or two cyano groups to the BT unit. Although, it should be noted that the V_{OC} of devices made from P(Ge-DTDCNBT) were quite varied, and the average was significantly lower (0.49 V) than the peak (0.68 V).

The most significant difference between the polymers was the large differences in J_{SC}. The substitution of one cyano group onto the BT unit of the polymer in P(Ge-DTCNBT) led to almost double the photocurrent exhibited by P(Ge-DTBT).

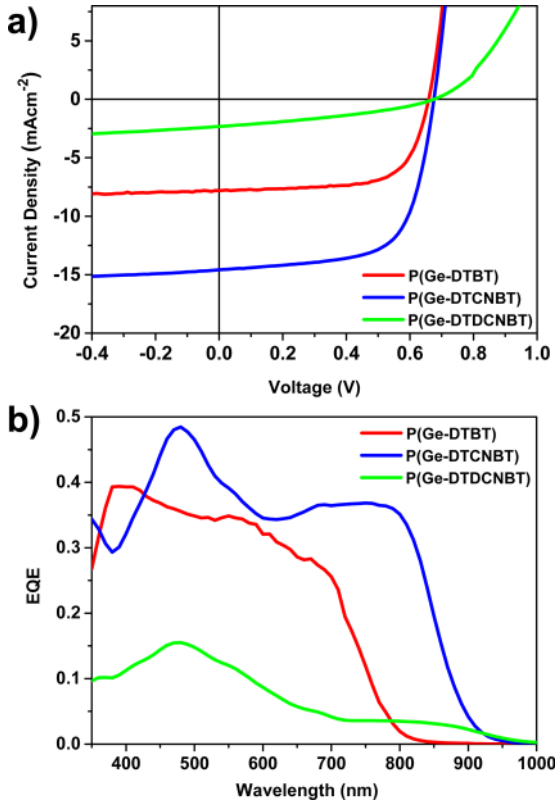

Figure 6. *J*−*V* curves (top) and EQE (bottom) of P(Ge-DTBT) (red), P(Ge-DTCNBT) (blue), and P(Ge-DTDCNBT) (green) blends with $PC_{71}BM$ (1:2).

However, the introduction of two cyano groups onto the BT unit of the polymer in P(Ge-DTDCNBT) led to a very low photocurrent of less than 3 mA cm^{-2}. The high J_{SC} exhibited by P(Ge-DTCNBT) is likely to be, in part, due to the optimization of the LUMO level energy, which led to a 0.16 eV reduction in the optical band gap of P(Ge-DTCNBT) compared to P(Ge-DTBT). The P(Ge-DTCNBT) devices absorb a greater percentage of the available solar flux, allowing a greater number of excitons to be formed in the film. As the quantum yield of the P(Ge-DTCNBT) device seemed to be relatively unchanged in comparison to the unsubstituted polymer P(Ge-DTBT), the greater number of excitons formed leads to a higher J_{SC}. The hole mobility of P(Ge-DTCNBT), measured in top gate/bottom contact organic field-effect transistor (OFET) devices, was also an order of magnitude higher than P(Ge-DTBT) (see Table 3). This may also help to explain the higher current measured in OPV devices made from P(Ge-DTCNBT), although the fill factor was not improved in comparison to P(Ge-DTBT).

The devices made using P(Ge-DTDCNBT) gave very low J_{SC}, with an average current of 2.42 mA cm^{-2}. According to the

DOI: 10.1021/acs.chemmater.6b02030
Chem. Mater. 2016, 28, 5110−5120

device EQE spectrum, the fullerene excitons in this blend contribute significantly more to the photocurrent than the polymer excitons. This lack of photocurrent generation by the P(Ge-DTDCNBT) excitons most probably derives from the low lying LUMO of the polymer that is comparable to $PC_{71}BM$, as we discuss further below. The negligible hole mobility of P(Ge-DTDCNBT) (measured in top gate/bottom contact OFET devices, see Table 3) will also contribute to the low J_{SC} measured, as even if excitons are able to separate the low hole mobility may result in a buildup of charges that will increase nongeminate recombination losses. This is also likely to explain the low fill factor (~0.3) measured for P(Ge-DTDCNBT) based devices.

Excited State Dynamics. To study the changes in J_{SC} between the reported devices, we carried out photoluminescence and ultrafast transient absorption spectroscopy studies of the three neat polymers and the corresponding P(Ge-DTBT):$PC_{71}BM$, P(Ge-DTCNBT):$PC_{71}BM$, and P(Ge-DTDCNBT):$PC_{71}BM$ (1:2) and (4:1) blends. From the data presented in Figure 7, we estimate that the polymer photoluminescence quenching in the P(Ge-DTBT):$PC_{71}BM$ and P(Ge-DTCNBT):$PC_{71}BM$ blends at both ratios is ~100%,

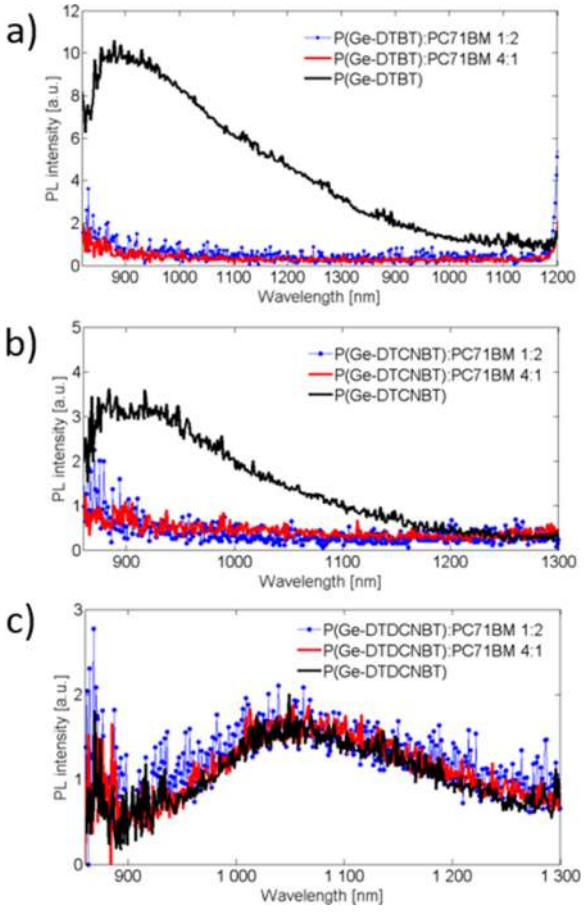

Figure 7. Photoluminescence spectra of P(Ge-DTBT) (a), P(Ge-DTCNBT) (b), and P(Ge-DTDCNBT) (c) films and P(Ge-DTBT):$PC_{71}BM$ (1:2), P(Ge-DTCNBT):$PC_{71}BM$ (1:2), and P(Ge-DTDCNBT):$PC_{71}BM$ (1:2) blends. The films were excited with 660 nm (a), 780 nm (b), and 820 nm (c) at the lowest energy absorption maximum of the polymers. The data shows strong PL quenching of P(Ge-DTBT) and P(Ge-DTCNBT) excitons but not of P(Ge-DTDCNBT) excitons in their corresponding blends.

meaning that all polymer excitons in the blend are dissociated due to the inclusion of fullerene electron acceptors. In contrast, for the P(Ge-DTDCNBT):$PC_{71}BM$ blend, no polymer fluorescence quench is observed within our sensitivity limits. Photoluminescence quenching is a good indicator of the exciton dissociation yields in polymer:fullerene blends and as such it allows us to suggest that poor exciton dissociation is the main reason behind the very low J_{SC} of the P(Ge-DTDCNBT):$PC_{71}BM$ device.[11,47] The likely reason for this inefficient exciton dissociation is the polymer's low LUMO level, which appears to be too low to drive electron transfer from the polymer to the fullerene. We also conclude that the addition of just one cyano group to the BT moiety in P(Ge-DTCNBT) leads to successful optimization of the polymer optical bandgap, providing improved light harvesting properties of the device for higher J_{SC} while still enabling efficient exciton dissociation.

Further studies of the charge generation dynamics of the three blends were carried out using femtosecond transient absorption spectroscopy in the NIR spectral region.[48−50] Figure 8 presents the transient absorption spectra of the neat polymer

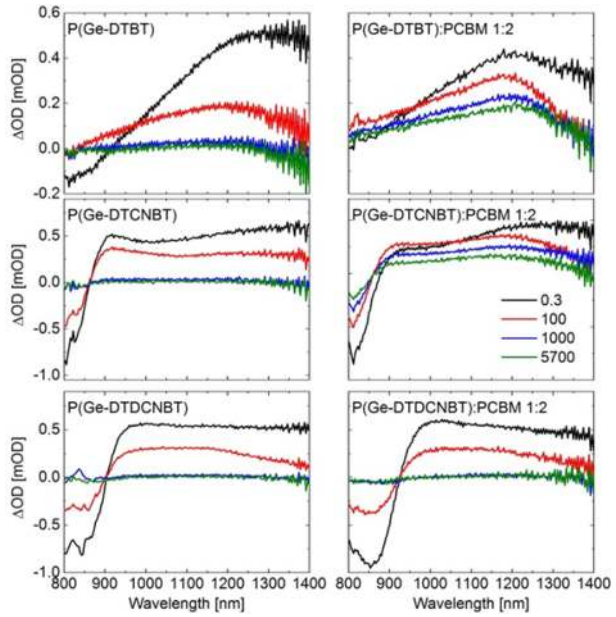

Figure 8. Ultrafast transient absorption spectra of the neat polymer (left column) and blend films (right column) recorded at 0.3 ps, 100 ps, 1000 ps, and 5700 ps after light excitation. The pump pulses exciting the samples had wavelengths as in Figure 7 and excitation densities between 5 and 20 μJ cm^{-2}.

films and the blends at four different delay times, recorded with pump pulses tuned to the lowest energy absorption maximum of the polymers and using low light densities to ensure a linear sample response. The negative signals in the spectra of the neat polymers correspond to stimulated emission in the case of P(Ge-DTBT) and ground state bleach in the case of P(Ge-DTCNBT) and P(Ge-DTDCNBT). The positive signals for all polymers are assigned to singlet exciton absorption, in agreement with other TAS studies of conjugated polymers.[51,52]

Exponential fitting of the singlet exciton decays therefore allows us to estimate that their lifetimes are as follows: $\tau_{P(Ge\text{-}DTBT)}$ = 109 ps, $\tau_{P(Ge\text{-}DTCNBT)}$ = 239 ps, $\tau_{P(Ge\text{-}DTDCNBT)}$ = 158 ps. It is apparent that the shorter exciton lifetime for P(Ge-DTBT) does not reduce the efficiency of exciton dissociation

DOI: 10.1021/acs.chemmater.6b02030
Chem. Mater. 2016, 28, 5110−5120

(as measured above from PLQ to be ∼100%), most likely due to significant fine mixing of fullerene into polymer rich domains reducing requirements for polymer exciton diffusion, as is often observed for polymer/fullerene blends.[53−57]

Turning our focus to the transient spectra of the P(Ge-DTBT):$PC_{71}BM$ and P(Ge-DTCNBT):$PC_{71}BM$ blends and comparing them to the spectra of the neat polymers, we identify that the blends and the neat films have completely different excited state absorption even after a 1 ps time delay (after excitation). We assign the new excited state absorption to polymer polarons based on additional microsecond transient absorption spectroscopy measurements (Figure S5) that show that the new states have microsecond lifetimes and power law decays typical of nongeminate polaron recombination,[58,59] as well as a complete lack of sensitivity to molecular oxygen (Figure S6). This assignment allows us to conclude that the polymer excitons in the P(Ge-DTBT):$PC_{71}BM$ and P(Ge-DTCNBT):$PC_{71}BM$ blends undergo very efficient exciton dissociation via electron transfer generating a high yield of charges. This conclusion is confirmed by the disappearance of the P(Ge-DTBT) stimulated emission from the spectra of P(Ge-DTBT):$PC_{71}BM$, which also indicates ultrafast exciton dissociation and charge generation.

These ultrafast processes are, however, not observed in the transient absorption spectra of P(Ge-DTDCNBT):$PC_{71}BM$, which we find is dominated by polymer exciton absorption. Furthermore, the lifetime of the polymer excitons in this blend are completely comparable with those of the neat polymer film, thus, providing further evidence that P(Ge-DTDCNBT) excitons are unable to dissociate via electron transfer at the polymer−fullerene interface and create very little if any charges in devices. The same conclusion is reached when looking at our microsecond TAS measurements of P(Ge-DTDCNBT):$PC_{71}BM$ which do not show any signals at the relevant excitation densities (Figure S7). Our ultrafast spectroscopy results therefore support our conclusion made from the photoluminescence quenching measurements and confirm that while the addition of two cyano groups to the BT moiety has an adverse effect on the charge generation properties of the P(Ge-DTDCNBT) polymer, due to its low LUMO level (−3.77 eV), the addition of just one cyano group optimizes the LUMO energy of P(Ge-DTCNBT) (−3.54 eV) for increased light harvesting and similarly high charge generation yields compared to P(Ge-DTBT) (−3.27 eV).

Previous spectroscopy results have shown that for some polymer/fullerene systems, the yield of dissociated charges is more sensitive to the magnitude of the LUMO−LUMO offset than the exciton quenching efficiency.[11] It has been proposed that high offsets are required to avoid exciton separation leading to the generation of intermediate bound/charge transfer states at the donor−acceptor interface that are more likely to undergo geminate recombination instead of dissociation to generate separated charges.[60,61] As such, several systems with modest energy offsets have been shown to exhibit efficient exciton separation, as measured by strong photoluminescence quenching, but more limited efficiencies of full charge dissociation and photocurrent generation due to such geminate recombination losses. Therefore, to further study the impact of energy offset in the three polymers synthesized here we recorded the polaron recombination dynamics in P(Ge-DTBT):$PC_{71}BM$ and P(Ge-DTCNBT):$PC_{71}BM$ on the nanosecond time scale (Figure S8) to probe the potential for geminate recombination losses. Our results show that charge geminate recombination channels are present in both blends and these lead to significant charge losses by 6 ns after photoexcitation. The geminate recombination loss however is not the same for the two systems; instead, the lower LUMO−LUMO offset P(Ge-DTCNBT):$PC_{71}BM$ blend has a bigger loss (52%) than the higher offset P(Ge-DTBT):$PC_{71}BM$ blend (∼40%). These geminate recombination losses are likely to be the primary reason for the relatively modest EQE values obtained for these blend films. The lowering of the LUMO level with the addition of 1 cyano group results in a modest increase in these geminate recombination losses, although this is outweighed by the improved light harvesting efficiency, leading to increased photocurrent generation. Overall, it is however notable that such geminate recombination losses are relatively modest in these blend films given the low LUMO level offset driving charge separation, which is a key factor behind the promising device efficiencies obtained with these polymer/fullerene blends.

CONCLUSIONS

We report the synthesis of the novel electron accepting monomer 4,7-bis(5-bromothiophen-2-yl)-5-cyano-2,1,3-benzothiadiazole bis-Br(DTCNBT) in which one cyano group is incorporated onto the 2,1,3-benzothiadiazole unit. The cyano group could be easily introduced through the nucleophilic aromatic substitution of the fluorine substituent of 4,7-bis(5-bromothiophen-2-yl)-5-fluoro-2,1,3-benzothiadiazole. Copolymerizing bis-Br(DTCNBT) with dithienogermole (DTG) yielded the donor−acceptor polymer P(Ge-DTCNBT) which was then compared to the analogous polymers containing the either the dicyano substituted BT acceptor unit (P(Ge-DTDCNBT)) or the unsubstituted BT unit (P(Ge-DTBT)). Incorporating the increasingly stronger electron accepting units was found to systematically lower the polymer frontier energy levels. The addition of each cyano group onto the BT unit was found to strongly lower the polymer LUMO level by ∼0.25 eV and weakly lower the polymer HOMO level by less than 0.1 eV (per cyano group). The optical and electrochemical band gaps of the polymers therefore decreased with the increasing strength of the electron accepting unit.

The OPV device efficiency of the polymers varied significantly, largely due to substantial differences in short-circuit current. The monocyano substituted BT polymer P(Ge-DTCNBT) had a peak power conversion efficiency of over 6.5%, almost double that of the unsubstituted BT polymer P(Ge-DTBT) (∼3.5%), while the efficiency of the dicyano substituted BT polymer P(Ge-DTDCNBT) dropped to less than 1%.

The changes in device performance were analyzed using transient absorption spectroscopy which was carried out with the polymer−fullerene blend films optimized during device testing. Our spectroscopy results reveal that the addition of cyano groups to the BT moiety leads to significant changes in charge generation properties between the three polymers. For the dicyano substituted polymer P(Ge-DTDCNBT), the reduction in LUMO level appears to eliminate almost completely the charge generation from polymer excitons, making the P(Ge-DTDCNBT):$PC_{71}BM$ device capable of generating photocurrent only through fullerene light harvesting. However, for the monocyano substituted polymer P(Ge-DTDCNBT), the reduction in LUMO level leads to improved light harvesting properties of the device without compromising on its polymer exciton dissociation yields. While some increase in charge geminate recombination is observed, this loss is just

DOI: 10.1021/acs.chemmater.6b02030
Chem. Mater. 2016, 28, 5110−5120

slightly higher than the loss in P(Ge-DTBT):$PC_{71}BM$ blends, thus making the P(Ge-DTCNBT) polymer the most efficient out of the series.

■ ASSOCIATED CONTENT

Supporting Information

The Supporting Information is available free of charge on the ACS Publications website at DOI: 10.1021/acs.chemmater.6b02030.

Experimental procedures and details; additional figures as mentioned in the text, including monomer and polymer NMR, FET plots, and transient absorption spectra (PDF)

■ AUTHOR INFORMATION

Corresponding Author

*E-mail: m.heeney@imperial.ac.uk.

Notes

The authors declare no competing financial interest.

Additional data relating to the paper can be found at doi.org/10.6084/m9.figshare.3479123.

■ ACKNOWLEDGMENTS

We thank the UK's Engineering and Physical Sciences Research Council (EPSRC) for financial support via the Doctoral Training Centre in Plastic Electronics (Grant EP/G037515/1) and the British Council (Grant Number 173601536).

■ REFERENCES

(1) Mazzio, K. A.; Luscombe, C. K. The Future of Organic Photovoltaics. *Chem. Soc. Rev.* **2015**, *44* (1), 78−90.

(2) Liu, Y.; Zhao, J.; Li, Z.; Mu, C.; Ma, W.; Hu, H.; Jiang, K.; Lin, H.; Ade, H.; Yan, H. Aggregation and Morphology Control Enables Multiple Cases of High-Efficiency Polymer Solar Cells. *Nat. Commun.* **2014**, *5* (9), 5293.

(3) Liu, C.; Yi, C.; Wang, K.; Yang, Y.; Bhatta, R. S.; Tsige, M.; Xiao, S.; Gong, X. Single-Junction Polymer Solar Cells with Over 10% Efficiency by a Novel Two-Dimensional Donor−Acceptor Conjugated Copolymer. *ACS Appl. Mater. Interfaces* **2015**, *7* (8), 4928−4935.

(4) Chen, J.-D.; Cui, C.; Li, Y.-Q.; Zhou, L.; Ou, Q.-D.; Li, C.; Li, Y.; Tang, J.-X. Single-Junction Polymer Solar Cells Exceeding 10% Power Conversion Efficiency. *Adv. Mater.* **2015**, *27* (6), 1035−1041.

(5) He, Z.; Xiao, B.; Liu, F.; Wu, H.; Yang, Y.; Xiao, S.; Wang, C.; Russell, T. P.; Cao, Y. Single-Junction Polymer Solar Cells with High Efficiency and Photovoltage. *Nat. Photonics* **2015**, *9* (3), 174−179.

(6) Chen, C.-C.; Chang, W.-H.; Yoshimura, K.; Ohya, K.; You, J.; Gao, J.; Hong, Z.; Yang, Y. An Efficient Triple-Junction Polymer Solar Cell Having a Power Conversion Efficiency Exceeding 11%. *Adv. Mater.* **2014**, *26* (32), 5670−5677.

(7) Zhou, H.; Zhang, Y.; Mai, C.-K.; Collins, S. D.; Bazan, G. C.; Nguyen, T.-Q.; Heeger, A. J. Polymer Homo-Tandem Solar Cells with Best Efficiency of 11.3%. *Adv. Mater.* **2015**, *27* (10), 1767−1773.

(8) Zhang, Z.; Wang, J. Structures and Properties of Conjugated Donor−Acceptor Copolymers for Solar Cell Applications. *J. Mater. Chem.* **2012**, *22* (10), 4178.

(9) Kularatne, R. S.; Magurudeniya, H. D.; Sista, P.; Biewer, M. C.; Stefan, M. C. Donor-Acceptor Semiconducting Polymers for Organic Solar Cells. *J. Polym. Sci., Part A: Polym. Chem.* **2013**, *51* (4), 743−768.

(10) Melkonyan, F. S.; Zhao, W.; Drees, M.; Eastham, N. D.; Leonardi, M. J.; Butler, M. R.; Chen, Z.; Yu, X.; Chang, R. P. H.; Ratner, M. a.; Facchetti, A. F.; Marks, T. J. Bithiophenesulfonamide Building Block for Π-Conjugated Donor−Acceptor Semiconductors. *J. Am. Chem. Soc.* **2016**, *138* (22), 6944−6947.

(11) Dimitrov, S. D.; Durrant, J. R. Materials Design Considerations for Charge Generation in Organic Solar Cells. *Chem. Mater.* **2014**, *26* (1), 616−630.

(12) Larson, B. W.; Whitaker, J. B.; Wang, X.-B.; Popov, A. A.; Rumbles, G.; Kopidakis, N.; Strauss, S. H.; Boltalina, O. V. Electron Affinity of Phenyl−C 61 − Butyric Acid Methyl Ester (PCBM). *J. Phys. Chem. C* **2013**, *117* (29), 14958−14964.

(13) Shahid, M.; Ashraf, R. S.; Huang, Z.; Kronemeijer, A. J.; McCarthy-Ward, T.; McCulloch, I.; Durrant, J. R.; Sirringhaus, H.; Heeney, M. Photovoltaic and Field Effect Transistor Performance of Selenophene and Thiophene Diketopyrrolopyrrole Co-Polymers with Dithienothiophene. *J. Mater. Chem.* **2012**, *22* (25), 12817.

(14) Uy, R. L.; Yan, L.; Li, W.; You, W. Tuning Fluorinated Benzotriazole Polymers through Alkylthio Substitution and Selenophene Incorporation for Bulk Heterojunction Solar Cells. *Macromolecules* **2014**, *47* (7), 2289−2295.

(15) Parker, T. C.; Patel, D. G.; Moudgil, K.; Barlow, S.; Risko, C.; Brédas, J.-L.; Reynolds, J. R.; Marder, S. R. Heteroannulated Acceptors Based on Benzothiadiazole. *Mater. Horiz.* **2015**, *2* (1), 22−36.

(16) Blouin, N.; Michaud, A.; Gendron, D.; Wakim, S.; Blair, E.; Neagu-Plesu, R.; Belletête, M.; Durocher, G.; Tao, Y.; Leclerc, M. Toward a Rational Design of Poly(2,7-Carbazole) Derivatives for Solar Cells. *J. Am. Chem. Soc.* **2008**, *130* (2), 732−742.

(17) Zhou, H.; Yang, L.; Price, S. C.; Knight, K. J.; You, W. Enhanced Photovoltaic Performance of Low-Bandgap Polymers with Deep LUMO Levels. *Angew. Chem., Int. Ed.* **2010**, *49* (43), 7992−7995.

(18) Li, W.; Yan, L.; Zhou, H.; You, W. A General Approach toward Electron Deficient Triazole Units to Construct Conjugated Polymers for Solar Cells. *Chem. Mater.* **2015**, *27* (18), 6470−6476.

(19) Yau, C. P.; Fei, Z.; Ashraf, R. S.; Shahid, M.; Watkins, S. E.; Pattanasattayavong, P.; Anthopoulos, T. D.; Gregoriou, V. G.; Chochos, C. L.; Heeney, M. Influence of the Electron Deficient Co-Monomer on the Optoelectronic Properties and Photovoltaic Performance of Dithienogermole-Based Co-Polymers. *Adv. Funct. Mater.* **2014**, *24* (5), 678−687.

(20) Ying, L.; Hsu, B. B. Y.; Zhan, H.; Welch, G. C.; Zalar, P.; Perez, L. A.; Kramer, E. J.; Nguyen, T.; Heeger, A. J.; Wong, W.; Bazan, G. C. Regioregular Pyridal[2,1,3]thiadiazole Π-Conjugated Copolymers. *J. Am. Chem. Soc.* **2011**, *133* (46), 18538−18541.

(21) Wang, M.; Wang, H.; Yokoyama, T.; Liu, X.; Huang, Y.; Zhang, Y.; Nguyen, T.-Q.; Aramaki, S.; Bazan, G. C. High Open Circuit Voltage in Regioregular Narrow Band Gap Polymer Solar Cells. *J. Am. Chem. Soc.* **2014**, *136* (36), 12576−12579.

(22) Chaurasia, S.; Hung, W.; Chou, H.; Lin, J. T. Incorporating a New 2 H -[1,2,3]Triazolo[4,5- c]pyridine Moiety To Construct D−A−π−A Organic Sensitizers for High Performance Solar Cells. *Org. Lett.* **2014**, *16* (11), 3052−3055.

(23) Chaurasia, S.; Ni, J.-S.; Hung, W.-I.; Lin, J. T. 2 H -[1,2,3]Triazolo[4,5- c]pyridine Cored Organic Dyes Achieving a High Efficiency: A Systematic Study of the Effect of Different Donors and Π Spacers. *ACS Appl. Mater. Interfaces* **2015**, *7* (39), 22046−22057.

(24) Zhou, H.; Yang, L.; Stuart, A. C.; Price, S. C.; Liu, S.; You, W. Development of Fluorinated Benzothiadiazole as a Structural Unit for a Polymer Solar Cell of 7% Efficiency. *Angew. Chem., Int. Ed.* **2011**, *50* (13), 2995−2998.

(25) Bronstein, H.; Frost, J. M.; Hadipour, A.; Kim, Y.; Nielsen, C. B.; Ashraf, R. S.; Rand, B. P.; Watkins, S.; McCulloch, I. Effect of Fluorination on the Properties of a Donor−Acceptor Copolymer for Use in Photovoltaic Cells and Transistors. *Chem. Mater.* **2013**, *25* (3), 277−285.

(26) Fei, Z.; Shahid, M.; Yaacobi-Gross, N.; Rossbauer, S.; Zhong, H.; Watkins, S. E.; Anthopoulos, T. D.; Heeney, M. Thiophene Fluorination to Enhance Photovoltaic Performance in Low Band Gap Donor-Acceptor Polymers. *Chem. Commun.* **2012**, *48* (90), 11130−11132.

(27) Stuart, A. C.; Tumbleston, J. R.; Zhou, H.; Li, W.; Liu, S.; Ade, H.; You, W. Fluorine Substituents Reduce Charge Recombination and

DOI: 10.1021/acs.chemmater.6b02030
Chem. Mater. 2016, 28, 5110−5120

Drive Structure and Morphology Development in Polymer Solar Cells. *J. Am. Chem. Soc.* **2013**, *135* (5), 1806−1815.
(28) Li, H.; Koh, T. M.; Hagfeldt, A.; Grätzel, M.; Mhaisalkar, S. G.; Grimsdale, A. C. New Donor−π−acceptor Sensitizers Containing 5H-[1,2,5]thiadiazolo [3,4-F]isoindole-5,7(6H)-Dione and 6H-pyrrolo-[3,4-G]quinoxaline-6,8(7H)-Dione Units. *Chem. Commun.* **2013**, *49* (24), 2409−2411.
(29) Nielsen, C. B.; Ashraf, R. S.; Treat, N. D.; Schroeder, B. C.; Donaghey, J. E.; White, A. J. P.; Stingelin, N.; McCulloch, I. 2,1,3-Benzothiadiazole-5,6-Dicarboxylic Imide - A Versatile Building Block for Additive- and Annealing-Free Processing of Organic Solar Cells with Efficiencies Exceeding 8%. *Adv. Mater.* **2015**, *27* (5), 948−953.
(30) Kim, H. G.; Kim, M.; Clement, J. A.; Lee, J.; Shin, J.; Hwang, H.; Sin, D. H.; Cho, K. Energy Level Engineering of Donor Polymers via Inductive and Resonance Effects for Polymer Solar Cells: Effects of Cyano and Alkoxy Substituents. *Chem. Mater.* **2015**, *27* (19), 6858−6868.
(31) Wudarczyk, J.; Papamokos, G.; Margaritis, V.; Schollmeyer, D.; Hinkel, F.; Baumgarten, M.; Floudas, G.; Müllen, K. Hexasubstituted Benzenes with Ultrastrong Dipole Moments. *Angew. Chem., Int. Ed.* **2016**, *55* (9), 3220−3223.
(32) Camaioni, N.; Po, R. Pushing the Envelope of the Intrinsic Limitation of Organic Solar Cells. *J. Phys. Chem. Lett.* **2013**, *4* (11), 1821−1828.
(33) Leblebici, S. Y.; Chen, T. L.; Olalde-Velasco, P.; Yang, W.; Ma, B. Reducing Exciton Binding Energy by Increasing Thin Film Permittivity: An Effective Approach To Enhance Exciton Separation Efficiency in Organic Solar Cells. *ACS Appl. Mater. Interfaces* **2013**, *5* (20), 10105−10110.
(34) Casey, A.; Han, Y.; Fei, Z.; White, A. J. P.; Anthopoulos, T. D.; Heeney, M. Cyano Substituted Benzothiadiazole: A Novel Acceptor Inducing N-Type Behaviour in Conjugated Polymers. *J. Mater. Chem. C* **2015**, *3* (2), 265−275.
(35) Amb, C. M.; Chen, S.; Graham, K. R.; Subbiah, J.; Small, C. E.; So, F.; Reynolds, J. R. Dithienogermole As a Fused Electron Donor in Bulk Heterojunction Solar Cells. *J. Am. Chem. Soc.* **2011**, *133* (26), 10062−10065.
(36) Small, C. E.; Chen, S.; Subbiah, J.; Amb, C. M.; Tsang, S.-W.; Lai, T.-H.; Reynolds, J. R.; So, F. High-Efficiency Inverted Dithienogermole−thienopyrrolodione-Based Polymer Solar Cells. *Nat. Photonics* **2011**, *6* (2), 115−120.
(37) Constantinou, I.; Lai, T.-H.; Zhao, D.; Klump, E. D.; Deininger, J. J.; Lo, C. K.; Reynolds, J. R.; So, F. High Efficiency Air-Processed Dithienogermole-Based Polymer Solar Cells. *ACS Appl. Mater. Interfaces* **2015**, *7* (8), 4826−4832.
(38) Pilgram, K.; Skiles, R. D. Synthesis of 2,1,3-Benzothiadiazole-carbonitriles. *J. Heterocycl. Chem.* **1974**, *11* (5), 777−780.
(39) Shao, J.; Chang, J.; Chi, C. Linear and Star-Shaped Pyrazine-Containing Acene Dicarboximides with High Electron-Affinity. *Org. Biomol. Chem.* **2012**, *10* (35), 7045−7052.
(40) Casey, A.; Ashraf, R. S.; Fei, Z.; Heeney, M. Thioalkyl-Substituted Benzothiadiazole Acceptors: Copolymerization with Carbazole Affords Polymers with Large Stokes Shifts and High Solar Cell Voltages. *Macromolecules* **2014**, *47* (7), 2279−2288.
(41) Zhang, J.; Parker, T. C.; Chen, W.; Williams, L.; Khrustalev, V. N.; Jucov, E. V.; Barlow, S.; Timofeeva, T. V.; Marder, S. R. C−H-Activated Direct Arylation of Strong Benzothiadiazole and Quinoxaline-Based Electron Acceptors. *J. Org. Chem.* **2016**, *81* (2), 360−370.
(42) Tierney, S.; Heeney, M.; McCulloch, I. Microwave-Assisted Synthesis of Polythiophenes via the Stille Coupling. *Synth. Met.* **2005**, *148* (2), 195−198.
(43) Pommerehne, J.; Vestweber, H.; Guss, W.; Mahrt, R.; Bassler, H.; Porsch, M.; Daub, J. Efficient Two Layer Leds on a Polymer Blend Basis. *Adv. Mater.* **1995**, *7*, 551−554.
(44) Cardona, C. M.; Li, W.; Kaifer, A. E.; Stockdale, D.; Bazan, G. C. Electrochemical Considerations for Determining Absolute Frontier Orbital Energy Levels of Conjugated Polymers for Solar Cell Applications. *Adv. Mater.* **2011**, *23* (20), 2367−2371.
(45) Bredas, J.-L. Mind the Gap! *Mater. Horiz.* **2014**, *1* (1), 17−19.
(46) Min, J.; Zhang, Z.-G.; Zhang, M.; Li, Y. Synthesis and Photovoltaic Properties of a D−A Copolymer of Dithienosilole and Fluorinated-Benzotriazole. *Polym. Chem.* **2013**, *4* (5), 1467−1473.
(47) Ohkita, H.; Cook, S.; Astuti, Y.; Duffy, W.; Tierney, S.; Zhang, W.; Heeney, M.; McCulloch, I.; Nelson, J.; Bradley, D. D. C.; Durrant, J. R. Charge Carrier Formation in Polythiophene/Fullerene Blend Films Studied by Transient Absorption Spectroscopy. *J. Am. Chem. Soc.* **2008**, *130* (10), 3030−3042.
(48) Etzold, F.; Howard, I. A.; Forler, N.; Cho, D. M.; Meister, M.; Mangold, H.; Shu, J.; Hansen, M. R.; Müllen, K.; Laquai, F. The Effect of Solvent Additives on Morphology and Excited-State Dynamics in PCPDTBT:PCBM Photovoltaic Blends. *J. Am. Chem. Soc.* **2012**, *134* (25), 10569−10583.
(49) Ohkita, H.; Ito, S. Transient Absorption Spectroscopy of Polymer-Based Thin-Film Solar Cells. *Polymer* **2011**, *52* (20), 4397−4417.
(50) Cabanillas-Gonzalez, J.; Grancini, G.; Lanzani, G. Pump-Probe Spectroscopy in Organic Semiconductors: Monitoring Fundamental Processes of Relevance in Optoelectronics. *Adv. Mater.* **2011**, *23* (46), 5468−5485.
(51) Reid, O. G.; Pensack, R. D.; Song, Y.; Scholes, G. D. Rumbles, G. Charge Photogeneration in Neat Conjugated Polymers. *Chem. Mater.* **2014**, *26* (1), 561−575.
(52) Dimitrov, S.; Schroeder, B.; Nielsen, C.; Bronstein, H.; Fei, Z.; McCulloch, I.; Heeney, M.; Durrant, J. Singlet Exciton Lifetimes in Conjugated Polymer Films for Organic Solar Cells. *Polymers* **2016**, *8* (1), 14.
(53) Bartelt, J. A.; Beiley, Z. M.; Hoke, E. T.; Mateker, W. R.; Douglas, J. D.; Collins, B. A.; Tumbleston, J. R.; Graham, K. R.; Amassian, A.; Ade, H.; Fréchet, J. M. J.; Toney, M. F.; McGehee, M. D. The Importance of Fullerene Percolation in the Mixed Regions of Polymer-Fullerene Bulk Heterojunction Solar Cells. *Adv. Energy Mater.* **2013**, *3* (3), 364−374.
(54) Collins, B. A.; Gann, E.; Guignard, L.; He, X.; McNeill, C. R.; Ade, H. Molecular Miscibility of Polymer-Fullerene Blends. *J. Phys. Chem. Lett.* **2010**, *1* (21), 3160−3166.
(55) Guilbert, A. A. Y.; Schmidt, M.; Bruno, A.; Yao, J.; King, S.; Tuladhar, S. M.; Kirchartz, T.; Alonso, M. I.; Goñi, A. R.; Stingelin, N.; Haque, S. A.; Campoy-Quiles, M.; Nelson, J. Spectroscopic Evaluation of Mixing and Crystallinity of Fullerenes in Bulk Heterojunctions. *Adv. Funct. Mater.* **2014**, *24* (44), 6972−6980.
(56) Jamieson, F. C.; Domingo, E. B.; McCarthy-Ward, T.; Heeney, M.; Stingelin, N.; Durrant, J. R. Fullerenecrystallisation as a Key Driver of Charge Separation in Polymer/fullerene Bulk Heterojunction Solar Cells. *Chem. Sci.* **2012**, *3* (2), 485−492.
(57) Westacott, P.; Tumbleston, J. R.; Shoaee, S.; Fearn, S.; Bannock, J. H.; Gilchrist, J. B.; Heutz, S.; DeMello, J.; Heeney, M.; Ade, H.; Durrant, J.; McPhail, D. S.; Stingelin, N. On the Role of Intermixed Phases in Organic Photovoltaic Blends. *Energy Environ. Sci.* **2013**, *6* (9), 2756−2764.
(58) Shuttle, C. G.; O'Regan, B.; Ballantyne, A. M.; Nelson, J.; Bradley, D. D. C.; Durrant, J. R. Bimolecular Recombination Losses in Polythiophene: Fullerene Solar Cells. *Phys. Rev. B: Condens. Matter Mater. Phys.* **2008**, *78* (11), 1−4.
(59) Nelson, J. Diffusion-Limited Recombination in Polymer-Fullerene Blends and Its Influence on Photocurrent Collection. *Phys. Rev. B: Condens. Matter Mater. Phys.* **2003**, *67* (15), 1−10.
(60) Brédas, J.-L.; Norton, J. E.; Cornil, J.; Coropceanu, V. Molecular Understanding of Organic Solar Cells: The Challenges. *Acc. Chem. Res.* **2009**, *42* (11), 1691−1699.
(61) Bakulin, A. A.; Dimitrov, S. D.; Rao, A.; Chow, P. C. Y.; Nielsen, C. B.; Schroeder, B. C.; McCulloch, I.; Bakker, H. J.; Durrant, J. R.; Friend, R. H. Charge-Transfer State Dynamics Following Hole and Electron Transfer in Organic Photovoltaic Devices. *J. Phys. Chem. Lett.* **2013**, *4* (1), 209−215.

DOI: 10.1021/acs.chemmater.6b02030
Chem. Mater. 2016, 28, 5110−5120